PCCP

Accepted Manuscript

ROYAL SOCIETY OF CHEMISTRY

www.rsc.org/pccp

Journal Name

RSCPublishing

ARTICLE

NMR Studies of DNA Microcapsules Prepared By Sonochemical Methods

Cite this: DOI: 10.1039/x0xx00000x

Irena Reytblat[a,b], Keren Keinan-Adamsky[a], Jordan Chill[a], Hugo E. Gottlieb[a], Aharon Gedanken[a,b] and Gil Goobes[a]

Received 00th January 2014,
Accepted 00th January 2014

DOI: 10.1039/x0xx00000x

www.rsc.org/

DNA molecules were recently converted using ultrasonic irradiation into microcapsules that can trap hydrophobic molecules in aqueous solution. These DNA microcapsules are able to penetrate prokaryotic and eukaryotic cells, deliver drugs and transfer genetic information e.g. for protein expression into the host cells. DNA molecules of different sizes and structures can be assembled into spherical capsules, yet, the interactions that hold them together in these large structural constructs are unknown yet. In the current study, capsules prepared from a 12 bases double helix DNA were investigated using NMR spectroscopy. Solution NMR studies of the DNA emulsion reveal DNA molecules with perturbed structure with size similar to the precursor DNA based on diffusion NMR measurements. 2D NMR correlation measurements and chemical shift perturbation analysis show partial unzipping of AT base pairs in the centre of the modified duplex, freeing nucleoside bases to interact with other bases on other precursor molecules thereby facilitating aggregation. Slow tumbling of the microspheres renders them invisible in solution NMR spectra, therefore magic angle spinning NMR measurements are performed which provide with some limited evidence of the DNA in the microcapsules state.

Introduction

DNA molecules with selected sequences can now be manipulated to form smart two- and three-dimensional nanodevices by programmed self-assembly[1,2]. Alternatively, they can be readily converted by ultrasonic irradiation into an oil-in-water emulsion of nano to micro size capsules in a simple one step reaction. These DNA microcapsules are characterized by desired properties such as cell penetrability and resistance to enzymatic degradation[3].

Ultrasonic emulsification of biomolecules in binary solvent systems was first reported by Suslick and co-workers more than two decades ago. Bovine serum albumin was used to form an oil-in-water emulsion of suspended microspheres[4,5]. Recently, we have utilized this technique to encapsulate hydrophobic drugs in proteinacious microspheres and to deliver them into cells[6]. We have also extended the technique to form RNA and DNA emulsions yielding hydrophobic-solvent-filled nucleic acid spheres[7,3] and have also utilized the genetic information embedded in the capsule walls for expression of desired proteins inside human U2OS cancer cells and E. coli competent cells[3].

The physical properties of spheres made from long DNA and RNA chains are markedly different. While the RNA capsules are easily decomposable, the DNA capsules are very stable, withstanding drastic conditions such as high temperatures (90 ºC), a wide range of pH values (2-13) and treatment with DNAses[3]. DNA capsules themselves show variability in stability, size distribution and cell penetrability dependent on precursor DNA's chain length and structure.

The mechanism of sonochemical formation of proteinaceous microspheres[8-11] is believed to involve crosslinking of S-S bonds between cysteine residues on different protein molecules[12]. For the polynucleic acid capsules, experimental evidence is still missing to determine which interactions hold together molecules in this state. We have recently proposed that the conversion of single stranded DNA into microspheres is stabilized by electrostatic interactions while the conversion of long double stranded DNA (ds-DNA) is prompted by new covalent bond formation however further details of nucleic acids residues that are involved in the interaction is missing[3].

In this study, physical properties of DNA capsules in emulsions made from short ds-DNA (Dickerson sequence) by ultrasonic irradiation are examined by light microscopy, light scattering and by NMR, ex situ. Solution NMR measurements of sonicated ds-DNA show that a slightly perturbed structure of the coiled DNA is formed due to exposure to the intense irradiation. This modified structure exhibits narrow lines that are resolvable and slightly shifted from the original Dickerson DNA lines giving evidence that no covalent bonds are dissociated and no new ones formed. Diffusion NMR measurements show that the species formed has a similar diffusivity and therefore size to the original ds-DNA. 2D solution NMR measurements on the perturbed and original Dickerson DNA molecules[12,13] allow us to assign the base peaks in the new formed structure, to analyse the chemical shift

changes residue-by-residue and translate them to localized structural distortions in the intermediate product, by comparing to previously reported chemical shift perturbations recorded during thermal denaturation of the same Dickerson DNA molecule.

The DNA duplex is shown to acquire a distortion mainly in the AT segment in the centre of the oligomer which resembles the initial coil fraying observed upon DNA melting. The unwinding of the coil in the intermediate structure, by the ultrasonic waves, can induce the assembly into the aggregated spherical form.

Comparing the overall line intensity in ^{1}H solution spectra before and after sonication shows that a fraction of the intensity is missing. This intensity is associated with protons in the capsule which cannot be detected by solution NMR. ^{1}H and ^{13}C NMR magic angle spinning (MAS) NMR spectra of the emulsion, following removal of excess solvent, show susceptibility broadened sideband manifolds of encapsulated dodecane and weak lines in the ^{13}C spectra associated with sugar carbon resonances in the DNA capsules.

Results and Discussion

Dickerson double helix DNA (d5'CGCGAATTCGCG)$_2$ in 1000:3 water:dodecane (v/v) mixtures irradiated with ultrasonic waves produce monophasic emulsions of DNA spheres with the hydrophobic solvent trapped inside the microspheres (oil in water emulsion). These DNA emulsions are typically stable over long periods of time. NMR measurements and optical images recorded after storage at 4 °C for periods of 1-3 months produced consistent results with the ones presented hereafter. The light microscope image in Figure 1A is a representative example of the DNA spheres that are formed in a wide range of sizes. Analysis of the image yields a size distribution of the spheres, shown in Figure 1B, which extends from hundreds of nanometers to several microns and reaches a maximum at 750 nm.

The size distribution of the DNA spheres in solution, measured using dynamic light scattering (DLS) and shown in Figure 1s in the supporting information, is consistent with the one shown in Figure 1.

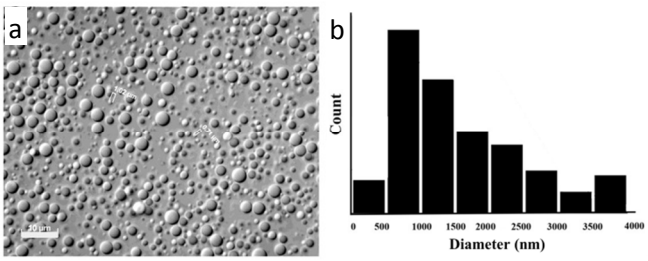

Fig. 1 (a) A representative light microscope image of freshly prepared Dickerson DNA spheres. **(b)** Size distribution analysis of Dickerson DNA spheres shown in the light microscope image on the left. The sphere size is given by its diameter.

The emulsions made from Dickerson DNA oligomers can be reversibly shattered and re-formed. To investigate the assembly of the DNA molecules into spheres, ^{1}H NMR measurements (shown in Figure 2) were carried out on the double helix DNA precursor (bottom) and the emulsion solution formed after the sonication (top). The spectrum of the emulsion shows narrow sugar and nucleoside lines, most of which are shifted with respect to the same lines in the original molecule, demonstrating that an intermediate DNA species is formed in solution after the treatment with the ultrasonic waves. This spectrum is representative of most preparations reflecting an efficient conversion of precursor molecules into the intermediate. A control ^{1}H NMR experiment on the Dickerson DNA sample dissolved in the aqueous phase of the water:dodecane biphasic discontinuous mixture without sonication gave a spectrum similar to that of the precursor (bottom spectrum) with negligible amounts of the intermediate. Resonances from the DNA microcapsules are not detectable using solution NMR experiments due to their slow tumbling in solution.

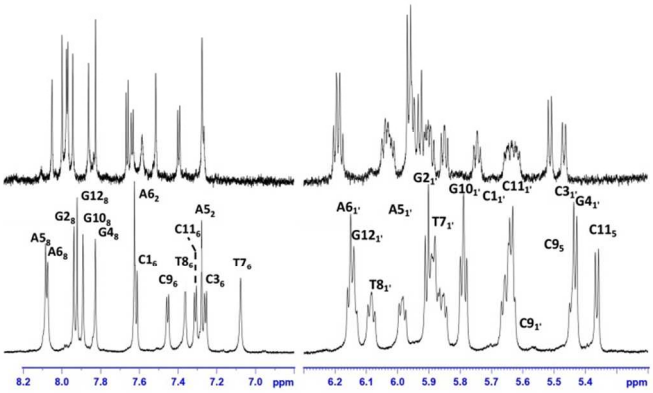

Fig. 2 The base protons H2, H6, H8 (left) and H5, H1' (right) regions in the ^{1}H-NMR spectra of Dickerson's DNA in its native form (bottom) and in the intermediate ds-DNA structure formed by sonication (top).

Further comparison of the DNA precursor and intermediate structures is done utilizing standard notation. The residue name (A, G, C or T) is followed by its position along the sequence counting from the 3' end and followed by a digit in subscript which shows the position of H or C in the molecule as shown in Figure 7; e.g. $A6_2$ is either C or H atom found at position 2 along the adenosine base of adenine residue 6. A detailed scheme showing atom numbering along the nucleosides and sugar ring is given in figure S2 in the supporting information. The resonances of H2, H6, H8 on the bases (6.8-8.3 ppm) and H1', H5 on the sugar rings (5.2-6.3 ppm) in the ^{1}H spectra of the ds-DNA (bottom) and the intermediate species formed (top) are shown in Figure 2. The proton shifts in the bottom spectrum are consistent with previously recorded spectra[13-16] but better resolved due to the high magnetic field (16.44 T) used here, allowing a straightforward assignment of ^{1}H peaks in the ds-DNA precursor spectrum. The intermediate's spectrum shows many of the peaks shifted and requires re-assignment for further analysis.

The ^{1}H-^{13}C HMQC (top) and ^{1}H-^{1}H NOESY (bottom) spectra of the Dickerson ds-DNA (black) and intermediate species (red) are shown in Figure 3. Assignment of the peaks for the intermediate was achieved by performing backbone walks on the NOESY spectrum as shown in Figure 3 along with the derived peak assignment. The changes observed in base proton positions between the precursor and the product intermediate along the dodecamer sequence are summarized in Figure 4 and Table S1 in the supporting information. The relatively small shifts in the base and sugar proton resonances indicate that formation of the intermediate does not involve dissociation of covalent bonds or formation of new ones.

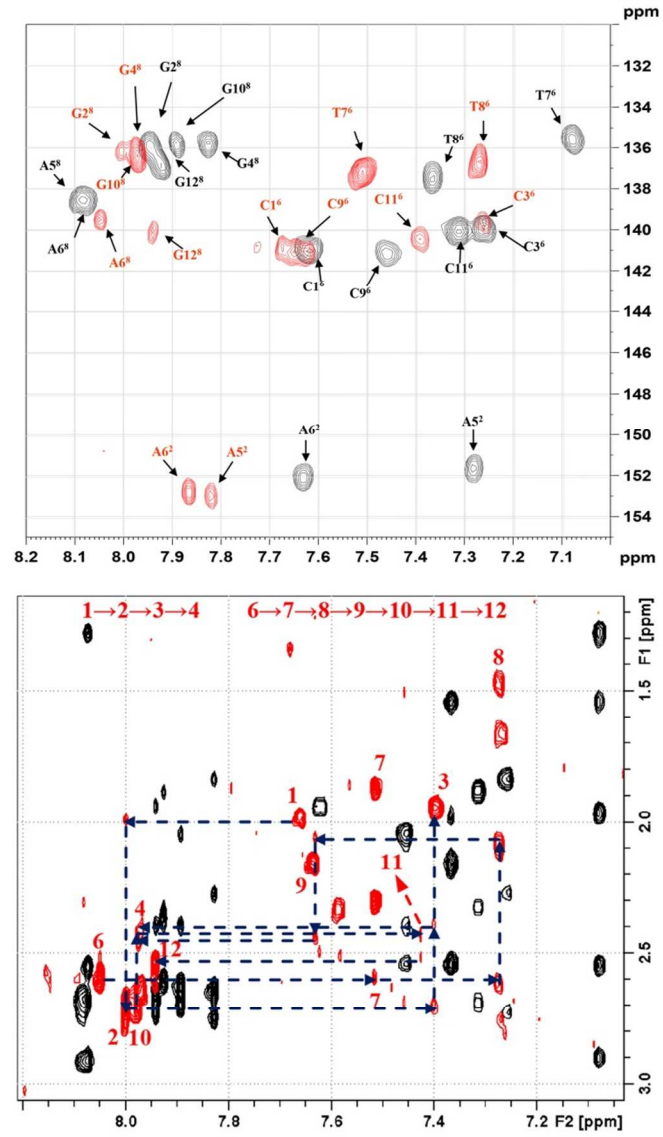

Fig. 3 (top) Base proton region in the ^{1}H-^{13}C HMQC spectrum with one-bond correlation selected (native form in black, sonicated in red). As can be seen, the carbon signals are also shifted between the two forms. **(bottom)** section from the ^{1}H-^{1}H NOESY spectrum corresponding on the horizontal axis to H2, H6 and H8 7.0-8.2) and the 2'-methylene on the vertical axis (native form in black, sonicated in red).

All base protons but the $T8_6$ exhibit a downfield shift that is increasing from the edges towards the centre of the double helix structure. The H2 protons close to Watson-Crick bonds on A and T bases at the centre of the dodecamer experience the largest downfield shift upon emulsification. These shifts are larger than in GC base-pairs which contain one hydrogen bond more than AT base-pairs. Downfield shifts were observed before in base protons during ds-DNA thermal denaturation as the helical structure disentangles into a pair single stranded DNA monomers [13].

Ultrasonic emulsification of biomolecules occurs through induction of localized high temperature gradients [17]. The chemical shift perturbations observed in the intermediate can be associated with thermal changes in the molecule and can compared to similar changes occurring during thermal melting of the Dickerson duplex[13]. Comparing the resonance changes reported in Table s1 in the supporting with resonance shifts observed in Dickerson duplex as the temperature is raised shows that no single temperature can be assigned to each and every deviation in resonance frequencies along the sequence but rather that the centre is characterized by a higher effective temperature than the tails.

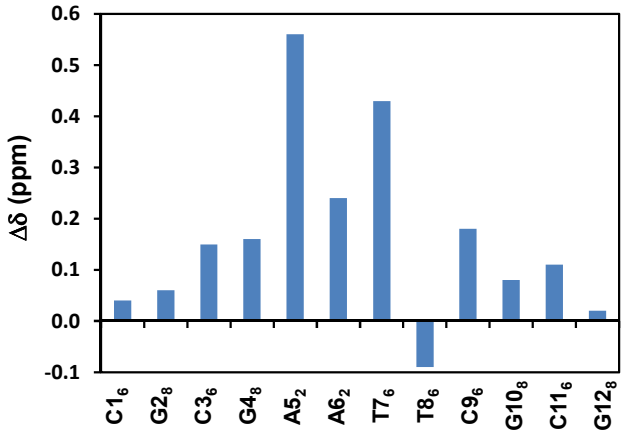

Fig. 4 Chemical shift difference between base protons in intermediate product and double helix precursor along the dodecamer.

These chemical shift perturbations between the intermediate species and the ds-DNA precursor in the centre residues (A5-T8) are equivalent to a helix denaturation already taking place while the chemical shift perturbations in the tails, on G1, C2, G10, C11 and G12, are equivalent to a moderate temperature rise where denaturation has not occurred yet. Denaturation of the ds-DNA involves complete helix fraying which requires weakening of all hydrogen bonds, and base de-stacking. Thus, the temperature gradients experienced by the ds-DNA due to the acoustic cavitation are sufficient to promote base de-stacking in the centre of the molecule and disruption of the coil structure however they are insufficient for complete helix defraying. Microcapsules generated, in separate experiments, from single stranded Dickerson DNA precursor had different size, stability and did not exhibit an intermediate species in the ^{1}H solution spectrum (data not shown) supporting the conclusion that the ultrasonic irradiation did not melt the ds-DNA completely into single stranded form.

To examine further the molecular size of the perturbed structure intermediate, we utilized diffusion measurements. Diffusion ^{1}H NMR experiments were carried out separately on the ds-DNA and on the sonication product in solution of D2O: dodecane (1000: 3 v/v) using gradient amplitudes of 7 to 15 gauss/cm, $\delta = 2.4$ ms and $\Delta = 0.3$ s. Results of fitting log of the normalized ^{1}H line intensity versus the square of the gradient strength, assuming a mono-gaussian decay, are shown in Figure 5. Diffusion coefficients for the two DNA species, deduced from the slopes of the curves, are $D_{dsDNA} = 4.17(\pm 0.14)\times 10^{-6}$ cm^2/s and $D_{spheres} = 6.45(\pm 0.27)\times 10^{-6}$ cm^2/s. The diffusion coefficient of the precursor is similar to that reported in the literature for the Dickerson duplex in aqueous solution [13, 16].

The diffusion coefficient of the intermediate species is 35% higher than the precursor's, indicating that its molecular weight

and overall dimensions are comparable to that of the original molecule. The absence of slow diffusing higher molecular weight species imply that neither soluble duplex dimers nor longer clusters of the precursors contribute to the narrow resonance lines of the intermediate. Dodecane diffusion measured in the same experiment (see inset in Figure 5) shows a decay of Log the line intensity with square of the gradient strength typical for compartmental diffusion as is expected for the encapsulated organic solvent [18].

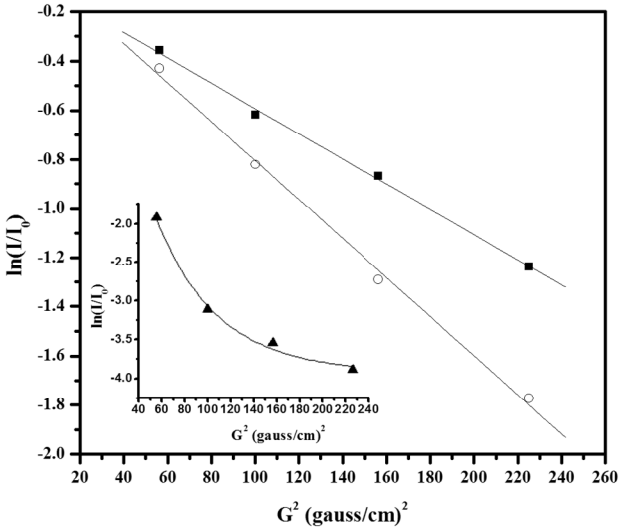

Fig. 5 ^{1}H Diffusion NMR results of dodecane-filled Dickerson DNA spheres (filled squares) and Dickerson double helix precursor (empty circles). Inset: ^{1}H Diffusion of dodecane (triangles) inside the DNA spheres showing restricted diffusion behaviour in the micron-size compartments.

To obtain spectral information of the DNA in the assembled form, we have carried out solid state NMR measurements on the microcapsules concentrated by removal of excess solvent. The ^{1}H MAS spectrum recorded at 1000 Hz (blue) is shown in Figure 6. It is compared to the solution spectrum of the precursor (red) in the inset of the Figure 6. Sideband manifolds of the solvent resonances (marked by *) are dominating the resonances from the DNA capsules. These large sidebands are a manifestation of susceptibility anisotropy caused by dodecane entrapment in the DNA microspheres. Similar effects were observed for other emulsion systems before [19]. The large susceptibility effects are observed also in the static ^{1}H NMR spectrum (blue) of the microcapsules (Figure S3 in the supporting information). Dodecane lines experience broadening and small resonance shift due to confinement [19]. The spectrum of the emulsion was recorded at a spinning rate of 5000 Hz, putting the dodecane sidebands outside the spectrum (see Figure S3 in the supporting information). However, clearer observation of proton resonances from the capsule was not achieved. At this spinning rate, it is also unclear whether the capsules remain intact.

^{13}C NMR measurement of the capsules, spun at 1800 Hz, provided with clearer evidence of sugar lines from the DNA microspheres. The spectrum, shown in Figure 7 reveals lines at 38, 45 and 47 ppm which coincide with the typical chemical shifts of C2' on C or T, C2' on G and C5' on A or C2' on G, respectively, as derived from the DNA chemical shift histograms deposited in the biological magnetic resonance bank [20]. The thymine methyl carbons in the aggregated DNA are masked by solvent peaks and the nucleoside lines are not observed.

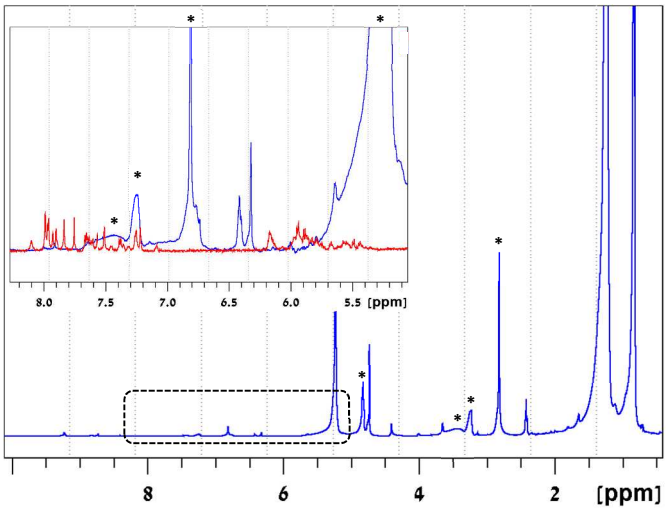

Fig. 6 ^{1}H MAS NMR spectra of DNA microcapsules spinning at 1000 Hz (blue) and in the inset a zoom-in of the spectrum on base and sugar region compared to precursor ^{1}H spectrum recorded in solution (red). Dodecane lines exhibit sideband manifolds denoted by * in the figure.

It is not entirely clear why only certain carbon and proton lines of the DNA in the capsule are observed and the rest are not visible, whether it is because a small number of ds-DNA molecules have assembled into microspheres, or related to motional broadening which renders these NMR resonances invisible both in solution and solid NMR measurements. The aggregated state of the DNA in the form of microcapsules is still quite challenging to characterize using solid state NMR and further studies using isotope enriched DNA and using high resolution magic angle spinning measurements are required to obtain details of building block packing in the assembled state.

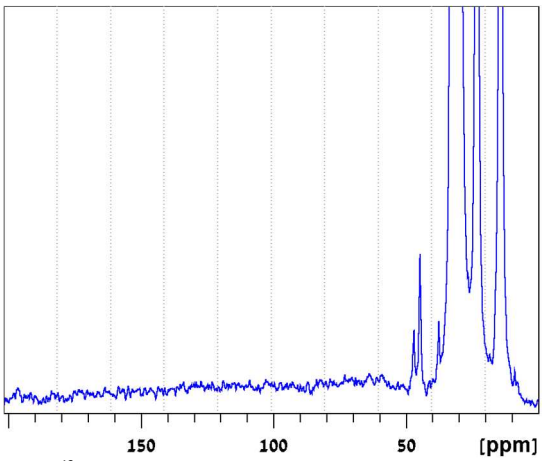

Fig. 7 ^{13}C spectrum of Dickerson DNA capsules spinning at 1800 Hz showing evidence for carbon resonances at 38-47 ppm on sugar rings in the aggregated DNA microcapsules.

The changes in the structure of the precursor ds-DNA are portrayed in Fig. 8 with the free A and T bases in the middle of the molecule, rotated out to allow them to interact with other duplex molecules as they assemble. The changes observed for Dickerson DNA depend strongly on its sequence and overall

structure therefore DNA molecules with different sequence or structure may undergo sonochemical emulsification in different ways than suggested here. Single stranded DNA molecules are found easier to convert into emulsions, however, their stability in aggregated microspherical form makes them less effective for the purpose of delivering their gene information following endocytosis. For the Dickerson duplex, the weak interactions which retain the DNA in microspherical state, as implied from the results shown here, are consistent with their ability convert back into active DNA form with external perturbation.

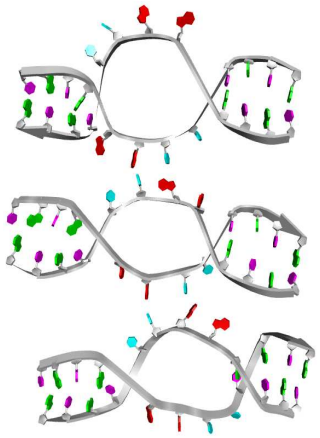

Fig. 8 A suggested model of the DNA structure distortion seen in the intermediate structure formed. Partial unzipping of AT pairs in the major groove of the Dickerson DNA and a subsequent base-pairing between distorted duplexes can promote aggregation to capsular structure. Cartoon made using ACCELRYS Discovery studio visualizer program.

Conclusions

In summary, emulsification of the Dickerson DNA dodecamer into microspheres is shown here to proceed through the formation of an intermediate structure as a result of the temperature gradients generated by the ultrasonic irradiation. The intermediate is characterized by dissociated Watson-Crick hydrogen bonds primarily between A-T bases in the centre of the DNA structure which have fewer inter-strand hydrogen bonds. Subsequently, base de-stacking and partial fraying of the helix in its centre can occur. The free bases can undergo excursions out of the major groove, allowing them to interact and participate in new H bonds across different duplex blocks thus facilitating assembly of the DNA into spheres.

Experimental

Preparation of Dickerson DNA microspheres

Microspheres were prepared by adding 6 µl of dodecane to an aqueous solution of the DNA prepared by dissolving 8mg of the Dickerson DNA (sequence 3'-CGCGAATTCGCG) in 2ml of doubly distilled H_2O. Sonication was performed for 3 min, and the cell was immersed in an ice bath, after which samples were taken for microscopy and NMR measurements.

NMR experiments

All solution NMR experiments were carried out using a 700 MHz Bruker Avance^{III} spectrometer and a cryogenic triple resonance TCI probe equipped with Z-axis gradient coils. ^{1}H and ^{13}C pulses at respective rf powers of 20.83 kHz and 17.8 kHz were employed in the NMR experiments. Decoupling of ^{13}C nuclei during ^{1}H acquisition in the ^{1}H-^{13}C HMQC experiment employed the GARP sequence. ^{1}H NOESY experiments employed 128 t_1 increments with a dwell time of 178.7 µs and a mixing time of 300 ms. A recycle delay of 4 s was used in all NMR measurements.

For the diffusion experiments, 8 mg of the Dickerson DNA were dissolved in a mixture of 1 ml D_2O and 6 µl dodecane and the sample was sonicated for 3 minutes. A pulsed field gradient sequence was employed for the diffusion measurements using a gradient duration of 2.4 ms and gradient separation of 0.3 s. Z-gradient power was varied between 7 and 15 Gauss/cm and the intensities of H2 and H6 lines were selected for diffusion measurement.

Solid NMR experiments were carried out on a 500 MHz Bruker Avance^{III} spectrometer using a 4 mm VTN CPMAS probe. ^{1}H spectra were acquired using rf power of 108.6 kHz and ^{13}C spectra using 40 kHz. Recycle delay of 5 s was used in these experiments.

Acknowledgements

This project was partially supported by an Israeli grant from the Ministry of Science, Technology and Space, grant No. 203253

Notes and references

[a] Department of Chemistry, Bar-Ilan University, Ramat-Gan 52900, Israel.

[b] Kanbar Laboratory of Nanomaterials Nanotechnology Research Center, Institute of Nanotechnology and Advanced Materials, Bar Ilan University, Ramat Gan 52900, Israel.

† Electronic Supplementary Information (ESI) available: [DLS data, static and spinning (5 kHz) ^{1}H spectra of capsules, scheme for DNA nomenclature, table of shifts in precursor and intermediate]. See DOI: 10.1039/b000000x/

1 P. W. K. Rothemund, *Nature,* 2006, **440**, 297-302.
2 H. Abe, N. Abe, A. Shibata, K. Ito, Y. Tanaka, M. Ito, H. Saneyoshi, S. Shuto, Y. Ito, *Angew. Chem. Int. Ed.* 2012, **51,** 6475- 6479.
3 U. Shimanovich, D. Eliaz, A. Aizer, I. Vayman, S. Michaeli, Y. Shav-Tal, A. Gedanken, *Chem. Bio. Chem.* 2011, **12,** 1678-1681.
4 K. S. Suslick, M. W. Grinstaff, *J. Am. Chem. Soc.* 1990, **112**, 7807-7809.
5 K. S. Suslick, M. W. Grinstaff, *Proc. Nat. Acad Sd. USA.* 1990, **88,** 7708-7710.
6 U. Shimanovich, A. Cavaco-Paulo, Y. Nitzan, A.Gedanken, *Chem. Eur. J.* 2012, **18,** 365-369.
7 U. Shimanovich, I. D. Tkacz, D. Eliaz, A. Cavaco-Paulo, S. Michaeli, A. Gedanken, *Adv. Funct. Mater.* 2011, **21,** 3659-3666.
8 F. Kratz, I. Fichtner, U. Beyer, P. Schumacher, T. Roth, H. H. Fiebig, *Eur. J. Cancer.* 1997**, 33,** 784-784.
9 C. Chevalier, A. Saulnier, Y. Benureau, D. Flchet, D. Delgrange, F. Colbre-Garapin, C. Wychowski, A. Martin, *Mol. Ther.* 2007**, 15,** 1452-1462.
10 R. Prabhu, R. F. Garry, S. Dash, *Virol. J.* 2006, *3*, 100-111.
11 A. Gedanken, *Chem. Eur. J.* 2008, **14,** 3840- 3853.

12 S. Avivi, A. Gedanken, *Biochem. J.* 2002, **366,** 705-707.
13 D. J. Patel, S. A. Kozlowski, L. A. Marky, C. Broka, J. A. Rice, K. Itakura, K. J. Breslauer, *Biochemistry* 1982, **21,** 428-436.
14 D. R. Hare, D. E. Wemmer, S. H. Chou, G. P. Drobny, B. R. Reid, *J. Mol. Biol.* 1983, **171,** 319-336.
15 E. Katsarou, A. Kolstad, N. Hadjiliadis, E. Sletten, *J. Inorg. Biochem.* 1998, **70,** 265-269.
16 N. J. Wheate, J. G. Collins, *J. Inorg. Biochem.* 2000, **78,** 313-320.
17 S. B. Barnett, G.R. Ter Haar, M.C. Ziskin, W.L. Nyborg, K. Maeda, J. Bang, *Ultrasound Med. Biol.* 1994, **20,** 205–218.
18 X. Li, J. C. Cox, R. W. Flumerfelt, *AIChE J.* 1992, **38,** 1671-1674.
19 J. H. Chen, B. M. Enloe, Y. Xiao, D. G. Cory, S. Singer, *Magn. Reson. Med.* 2003, **50,** 515-521.
20 E. L. Ulrich et. Al, *Nucl. Acids Res.* 2008, **36,** D402-D408.